New Application and Recent Improvement of Raman Spectroscopy

Yasushi NAKATA

Emmanuel FROIGNEUX

Raman spectroscopy have been progressed with new technologies applied to specific applications. By combining microscopy, its sensitivity has been increased as several orders in these decades. Especially, some new technologies for Raman imaging has been developed and will open new analytical world. In this report, we explain new Raman application of pharmaceutics, carbon materials (graphen and carbon nanotube), and lithium ion battery. In these, Raman analytical technology used in HORIBA products are also introduced.

Introduction

Since Delhaye introduced efficiency of microscopic system into Raman spectroscopy[1, 2], its sensitivity has improved several orders. As the results, micro-spectroscopic Raman system was widespread and still improving in the frontline of research fields. In this report, recent typical application and improvement of Raman spectroscopy will be introduced.

What is Raman Spectroscopy?

The vibrational Raman spectrum provides a fingerprint which characterizes chemical and molecular structure. The spectroscopic information can be regarded as similar in content, but often superior to that provided by Infra-Red (IR) spectroscopy, namely due to the much higher spatial resolution available through confocal Raman microprobes. As shown in Figure 1 Raman scattering is an inelastic light scattering process in which a laser photon is scattered by a sample molecule or crystal and loses energy during the process. The amount of energy loss is characteristic of the molecular bondings, thereby revealing the detailed nature of the investigated material. It enables highly specific chemical identification without ambiguity, in gas, liquid or solid phase, without requiring tedious and costly sample preparation.

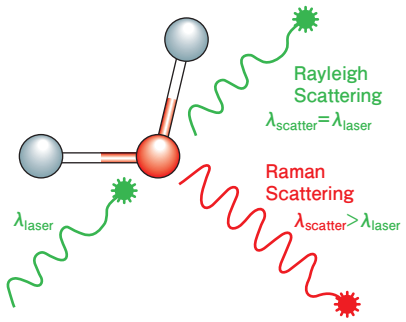

Figure 1 Principle of Raman scattering

Application to Evaluation of Pharmaceutical Compounds

Raman micro spectroscopy is a powerful and widely used analytical tool within the pharmaceutical industry. It is non-destructive, and offers fast versatile chemical identification. Combination with an optical microscope offers the advantage of analyzing minute material quantities (such as single grains or crystals) and the ability to monitor the distribution of components across a sample. Excipients and Active Pharmaceutical Ingredients (APIs) can be analyzed within seconds, and extensive Raman spectral libraries allow easy chemical identification. More subtle changes in structure such as polymorphism (in which a material can exist in more than one crystal form, even in the identical chemical composition) and crystallinity can be investigated using Raman spectroscopy. Both can have strong influence on drug dissolution and efficacy. Therefore understanding the true nature of an API is critical to the success of drug development and manufacture.

A key requirement for Raman is for tablet mapping,

which is widely used to assess tablet uniformity and investigate the distribution and grain size of excipients and APIs. Mapping areas can range from a full tablet (for a quick overview of the tablet) through to just a few tens of micrometers (for detailed analysis of individual grains and phase boundaries). New imaging technologies such as SWIFT and DuoScan allow these information rich maps to be acquired in minutes/hours rather than days/weeks as used to be the case until very recently. Raman fast mapping data from an aspirin containing painkiller are shown in Figure 2. Pharmaceutical tablets contain a number of components in addition to the API which is chosen for its therapeutic effects. These components are used to bulk out the tablet, provide lubrication during mixing and compaction, and aid digestion. Three Raman maps have been acquired, moving from a large area low resolution whole tablet image, through to a high resolution small area of interest to analyze individual grains/particles in detail. In the whole tablet map (1), which comprises 50,901 pixels over a 7 × 18 mm^2 area, the major constituents (aspirin, paracetamol and caffeine) are visible, in addition to the tablet coating. A higher resolution image (2) highlights a fourth component (cellulose) widely spread across the tablet, but present only in small, discrete areas. The final image (3) was acquired with 2 µm step (90,601 data points), and allows the size and shape of individual cellulose grains to be observed. Spectra from these four main components are also shown, illustrating the ease with which they can be distinguished using Raman.

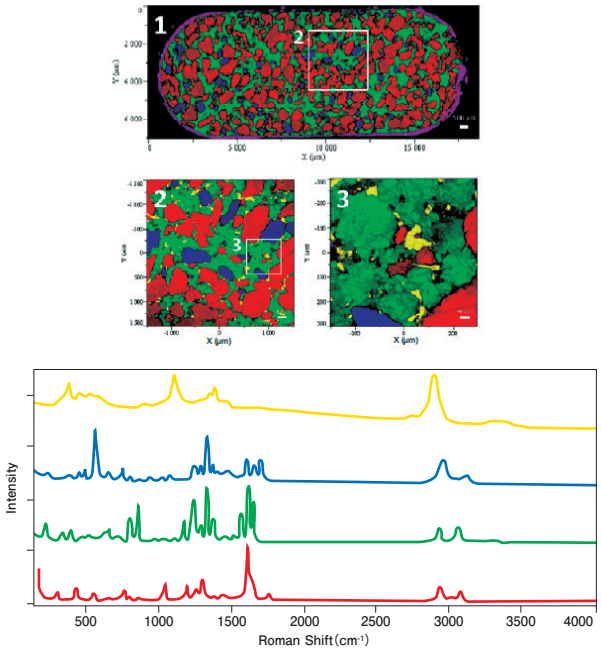

Figure 2 Color-coded Raman images of a pharmaceutical tablet highlighting the spatial distribution of the various components at different scales, allowing to explore the tablet uniformity as well the grain size and boundaries. The spectral signatures underneath are linked to the different chemical constituents. These results were measured by HORIBA Raman microscope XploRA,

Raman micro mapping is usually performed in backscattering configuration as surface measurement in high spatial resolution. It provides good statistical representation of the surface limited by the penetration depth of incident laser light. On the other hand, bulk analysis of content uniformity or polymorphism in pharmaceutical tablets is also available by Transmission Raman Spectroscopy (TRS)[3, 4]. As in classical Raman spectroscopy, TRS is non-contact, non-invasive and non-destructive. It requires no sample preparation. Importantly, the measurement is insensitive to particle-size effects, sample homogeneity and orientation. Therefore it provides good statistical representation of the whole sample. Figure 3 shows the comparison between Raman micro mapping and TRS for a two-layer tablet, consisting of API (propranolol) on one side and an excipient (mannitol) on the other, as an example of a tablet with non-uniform components distribution. Measurements were done on each side of the sample. In Figure 3(A), blue and red line spectra from the two sides are different, because Raman microscopy proved only surface. Because TRS analyses the incident light that traveled through the entire thickness of the sample, both spectra are the same as shown in Figure 3(B). It's an interesting solution for the routine analysis to get reliable information about API

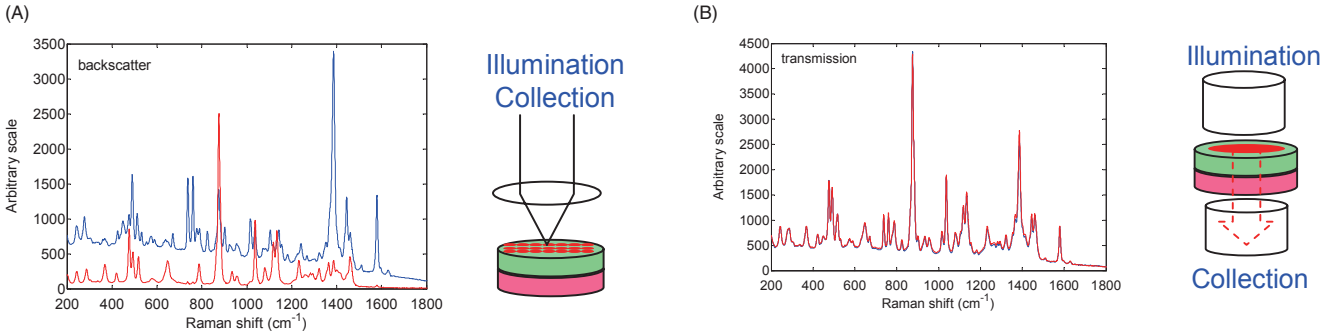

Figure 3 Comparison between Raman micro mapping (A) and TRS (B) for a two-layer tablet. Blue line is API side spectrum. Red line is expieut side spectrum.

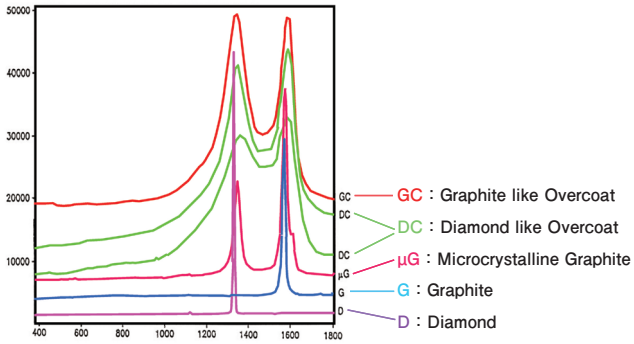

Figure 4 Raman spectra of diamond (D), graphite (G), microcrystalline graphite (μG), diamond like overcoat (DC), and graphite like overcoat (GC).

concentration, polymorphs analysis, crystallinity, powder composition/purity, content uniformity, and Solid form.

Application to Carbon Materials[5]

Different carbon materials are used in various engineering applications, from high tech to low tech. Carbon films are used as tribological coating; carbon fibers are used in composites for their strength; and nanotubes and graphene as nano-materials have been explored for use in microelectronics. Carbon composites have wide-ranging uses from aerospace to athletic gear. The ability of Raman spectroscopy to characterize these materials, in situ, with high spatial resolution (better than 1 μm) can be exploited during not only basic research, but also development and QC. The Raman spectra of the various allotropes of carbon are the best understood in the framework of solid-state physics. Diamond has the structure with two carbon atoms in the unit cell. All C-C bonds are tetrahedral (sp^3) and the lattice is cubic. The phonon frequency of diamond is 1332 cm^{-1}. Graphite is composed of stacks of planes of sp^2-bonded carbon. There are two doubly degenerate, Raman-active, in plane, E_{2g} modes, with frequencies of 1582 and 42 cm^{-1}, the former being known as the "G" mode. The lower frequency mode corresponds to shear motion of the two planes and can only be observed in instruments capable of recording frequencies well below 100 cm^{-1}. If one grinds graphite into smaller crystallites, a "disorder" or D band appears somewhere in the vicinity of 1280 and 1400 cm^{-1}, depending upon the excitation wavelength[6, 7]. Typical spectra of carbon are introduced in Figure 4. Variation of Carbon spectra with D and G bands in sp^2-bonded carbon are observed between crystalline states. For comparison, diamond spectrum is also shown in it.

The Raman spectra of graphene, a single layer of graphite, and a finite number of graphene layers also have been studied[8]. Typical single and multi-layer graphene spectra are shown in Figure 5. In the spectrum of a single layer

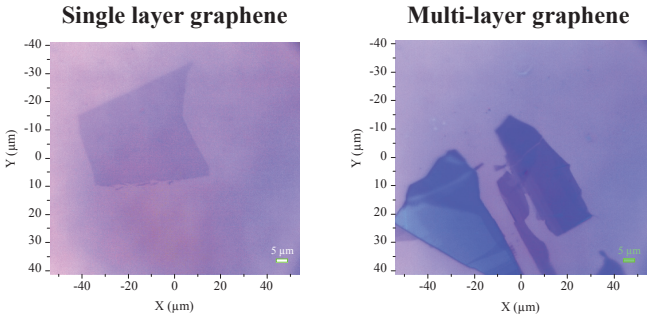

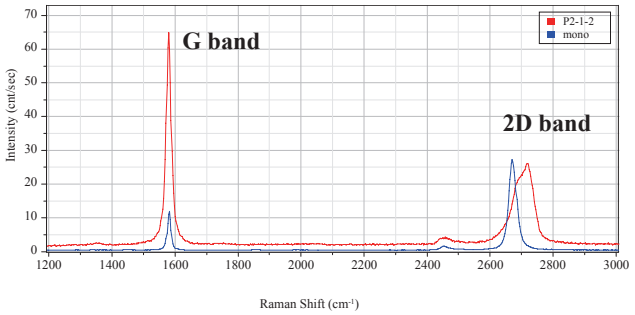

Figure 5 Raman spectra of single layer and multi-layer graphene

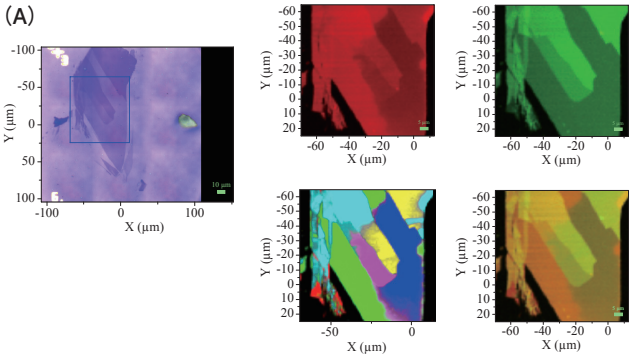

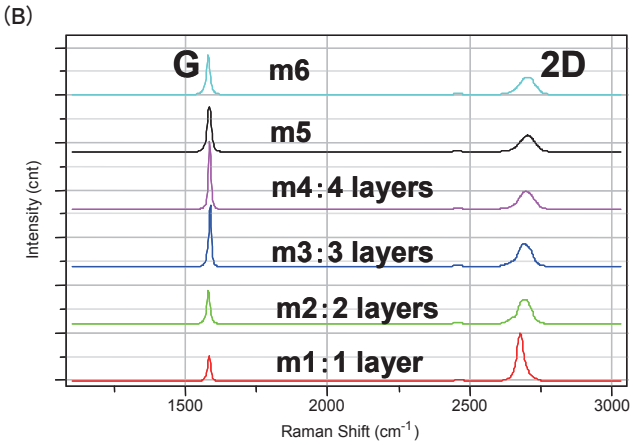

Figure 6 Ruman mapping of a graphene fragment
(A) Raman imaging: The blue rectangle in video image (left) is the mapping area. Intensity distributions of 2D (red) and G (green) bands and the overlay image of two are shown in Raman images (right). Multi-colored image is score image of extracted spectra of (B) by multivariate analysis. Colors of the images are red (m1), green (m2), blue (m3) , purple (m4), yellow (m5) and cyan (m6). (B) Loading spectrum extracted by multivariate analysis.

of graphene, the 2D band near 2700 cm^{-1} is several times as intense as the G band. A bilayer has a much broader and up-shifted 2D band with respect to graphene. When there is more than one graphene layer, the relative intensity of G band to 2D bands depends upon the number of layer (up to five layers). Because of this, the Raman spectrum can be used to determine the number of layer of graphene in a film of five or fewer layers. In Figure 6, the spectra, which were automatically extracted from mapping data of few layers graphen fragment. The ratio of G and 2D band intensity of graphenes was increasing from single to four layers. Recently, HORIBA ULF ultra low frequency module makes it possible to measure the shear mode of multilayer graphene with an efficient single stage spectrometer[9]. This Raman band scales from ~43 cm^{-1} in bulk graphite to ~31 cm^{-1} in bilayer graphene. Figure 7 shows low-frequency Raman bands of share mode of few-layer graphene by Raman micro-spectroscopy with ultra low frequency module.

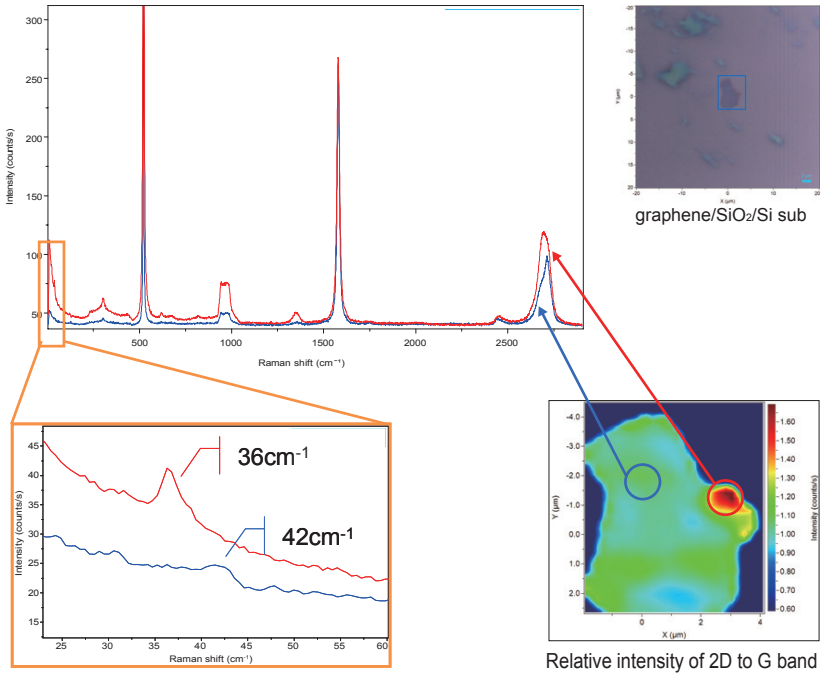

Figure 7 Share mode of few-layer graphene by Raman micro-spectroscopy with ultra low frequency module

Atomic Force Microscopy (AFM) is also strong tool to evaluate thickness of graphene. By using HORIBA coupling system of AFM and Raman mapping system, both topography and Raman image for graphene at the same area are successfully measured (see Figure 8). Macro-mapping mode of HORIBA DuoScan module as described bellow is a good way of performing survey scans to find small objects over a large surface. Once a region of interest has been identified within the sample, a more accurate mapping can be performed in step-by-step mode. In Figure 9, we searched for isolated Single-Wall Carbon Nanotubes (CNTs) grown parallel to one another on a Silicon sample. The CNTs are about 1 nm in width and are separated by about 500 µm. Figure shows macro-scale image of the sample (full width >1 mm) obtained in macro-mapping mode. The colors correspond to the integrated intensity of the Si band (red) and of the respective G bands of the CNTs (green and blue). Once the CNT of interest has been located, a high-definition image of the CNT is then obtained by zooming in with DuoScan in step-by-step micro-mapping mode (inset). In that case, the apparent width of the CNT (366 nm) is a convolution of the tube diameter with the laser spot size. This shows the superior spatial resolution achievable with a confocal microscope.

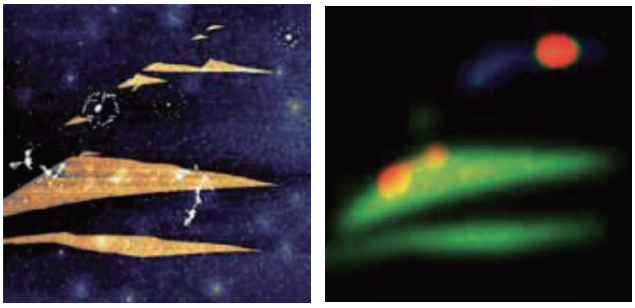

20 µm×20 µm AFM Topography
Height range 3 nm

Raman map G band (green),
2D band (red).

Figure 8 Topography and Raman image of graphene
(Courtesy of Prof. Lukas Eng's group, IAAP, Dresden, Germany.)

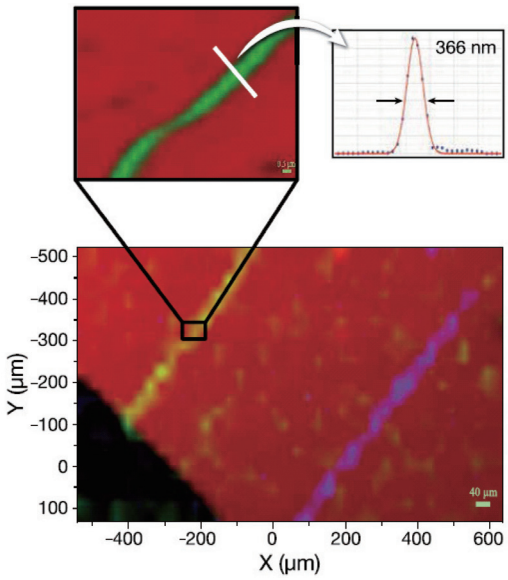

Figure 9 Macro-map and zoomed-in step-by-step map of a CNT obtained with DuoScan. (Sample courtesy of Dr. Kalbac, Heyrovský Institute, Czech Republic)

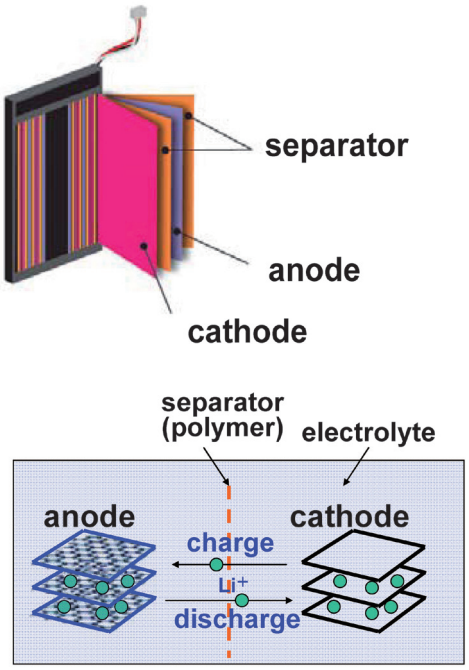

Figure 10 Structure of LIB

Lithium Ion Battery

Lithium Ion Batteries (LIB) have been widely used to power portable electronic equipments, and have long been considered as possible power sources for electronic or hybrid vehicles. Figure 10 shows structure of LIB which is constructed with cathode, anode and electric separator. LIB cell is filled with electrolyte.

Cathode materials play an important role on determining performances of lithium ion batteries. $LiCoO_2$(LCO) is the most popular cathode material so far used in lithium-ion batteries since its first introduction by Sony in 1990[10].

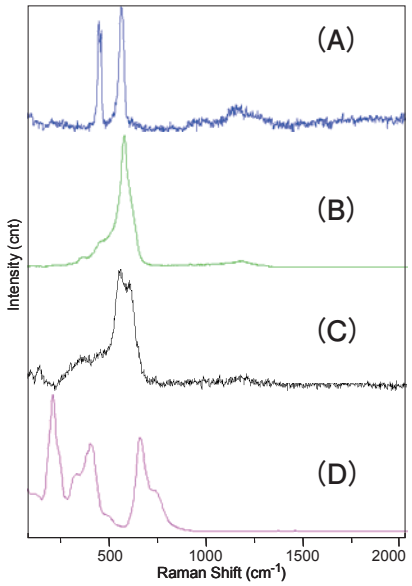

Figure 11 Raman spectra of cathode materials
(A) $LiCoO_2$, (B) Li (Ni, Mn, Co) O_2, (C) $LiMn_2O_4$, (D) Li_2TiO_3

Currently, new cathode materials (layer transition-metal oxide) were proposed as an alternative to LCO[11]. They can provide higher reversible capacity, lower material cost, and milder thermal stability. Figure 11 shows Raman spectra of cathode materials. Prolonging the LIB lifetime and its degradation mechanism remain important objective for battery research. 10-15 years of battery lifetime is required for transportation application. It is known that LCO change into cobalt oxide CoO_2 in a degradation LIB. The surface of washed cathode electrode picked up from LIB after long cycle test was evaluated by Raman mapping. CoO_2 Raman band was detected with LCO Raman bands. In the Raman image of Figure 12, red region of CoO_2 was clearly found near blue region of LCO particles.

Graphite material used for anode in common LIB. It is important to evaluate deterioration of graphite which is related to prolong battery lifetime. To quote Sethuraman et al. in their report (introduction of ref.[12]), "Though several different anode chemistries are currently pursued, graphite is still the primary choice for anodes used in commercial lithium-ion batteries. However, graphite anodes suffer severe surface structural disordering upon prolonged cycling in rechargeable lithium-ion batteries. This deleterious effect is intensified at high charging rates and elevated temperature as evidence in the Raman spectra of graphite anodes sampled from aged/cycled

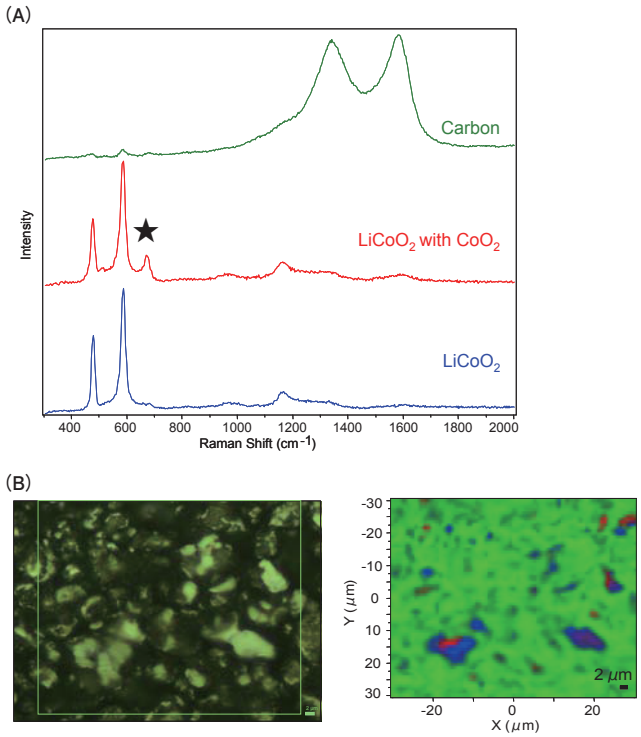

Figure 12 Raman mapping of cathode electrode
(A) Loading spectra extracted from mapping data.
★ : Raman band of CoO_2
(B) Video image and Raman score image. Green rectangle is mapping area. Colors of region are corresponded to loading spectra.

lithium-ion cells, which show an increased intensity of the carbon D-band (ca. 1350 cm^{-1}) with respect to the G-band (ca. 1580 cm^{-1}). This surface structural disorder is continuously inflicted on the graphitic crystallites in the anode upon prolonged charge/discharge cycling, modifies their electrocatalytic properties, and consequently, affects the thickness and composition of the solid-electrolyte-interphase (SEI) layer. The continuous reduction of the electrolyte and reformation of the SEI layer results in the gradual loss of cyclable lithium and consumption of the electrolyte. Since lithium is a finite resource in a typical lithium-ion battery, this loss is directly responsible for its capacity fade, and eventual failure."

Raman mapping image in Figure 13(A) shows the distribution of graphite 1 and graphite 2 as green and blue regions respectively and anode binder of fluorocarbon resin as red region. The ratio of D band intensity to G band for graphite 1 and graphite 2 in Figure 13(B) reflects the degree of clistallinity. Therefore, The Raman image shows the distribution of graphite crystallinity. Raman spectroscopy can be applied to in situ measurement without contact and any sample preparation. By using sealed cell (see Figure 14), LIB is sealed in argon gas environment. During charge/discharge cycle test, Raman laser probe can access the electrode surface directly through quartz window of this sealed cell in atmospheric condition. Figure 15 shows the result of Raman measurement in this manner. This result shows that LCO Raman band was distinguished in charged state.

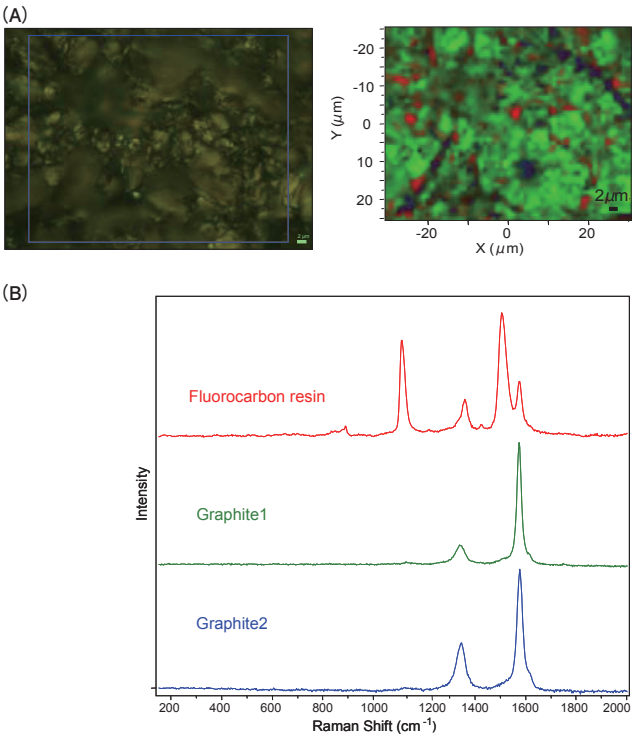

Figure 13 Raman mapping of anode electrode
(A) Video image and Raman score image. Blue rectangle is mapping area. Colors of region are corresponded to loading spectra.
(B) Loading spectra extracted from mapping data

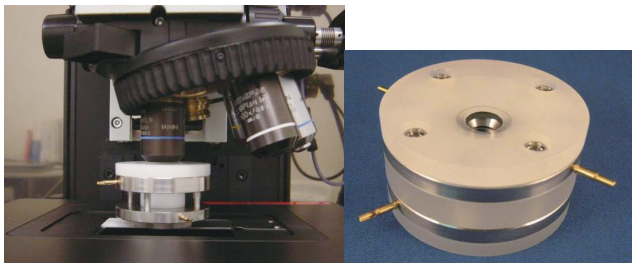

Figure 14 Sealed cell for in situ Raman measurement of lithium-ion battery

Recent Improvement of Raman spectroscopy

The SWIFT ultra-fast Raman Imaging Module

Raman imaging is widely used to characterize the distribution of components within a sample, but additionally it is sensitive to material concentration, phase, stress/strain, and crystallinity. With a single data set a wide variety of Raman images can be created which take the researcher well beyond what the eye can see. Standard point-by-point mapping affords the ultimate sensitivity for materials with extremely low Raman scattering properties, and additionally allows high resolution and/or large spectral range capability. Typical acquisition times for such maps can be in the order of 1 s-10 s per point (or longer), and thus total measurement times can be significant. HORIBA SWIFT ultra-fast Raman

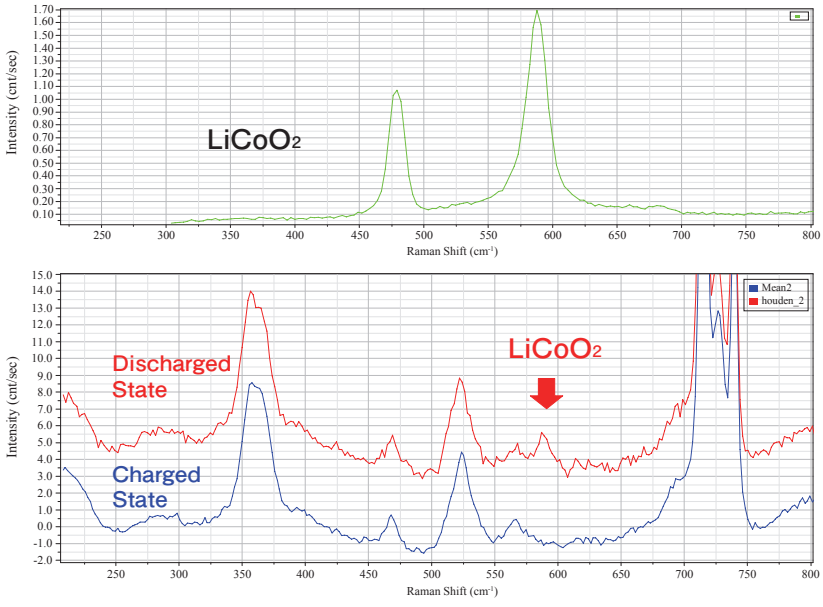

Figure 15 In situ Raman measurements of LIB charged and discharged state

Imaging module[13] offers drastically reduced measurement times with acquisition times down to <1 ms/point, allowing large area survey scans and detailed Raman images to be completed in seconds or minutes. Although not suitable for every sample, SWIFT heralds a new era in Raman mapping, combining quality Raman spectroscopy with high spatial resolution without compromise in measurement time.

The DuoScan Imaging Technology

Creating high quality, detailed Raman images requires good spatial resolution, and optimized configurations provide spatial resolution in the sub-micron regime. HORIBA true-confocal Raman microscope system offers high spatial resolution up to diffraction limit, with laser spot sizes typically focused down to 0.5 - 1 μm diameters, depending on the laser wavelength and focusing optics. The DuoScan Imaging technology[14] available on the instruments of the LabRAM Series introduces a new imaging mode, based on a combination of scanning mirrors that scan the laser beam in a pattern chosen by the operator: a line for linear profiles, or an area for two-dimensional mapping (see Figure 16). The use of scanning devices for mapping is usually limited to visible light since refractive elements placed on the beam path cannot be used outside this range. The DuoScan system extends this operational range, enabling mapping from the deep UV to the Infrared (in the limits of the microscope objective capabilities). Moreover, the unique combination of the DuoScan technique with True Confocal design allows the Raman microscope to scan very small sample areas or volumes with unsurpassed lateral and axial resolution. When looking at large sample surfaces, whether it is to measure component distribution or to search for contaminants, it often comes down to finding a needle in a haystack. In macro mapping mode of DuoScan, the laser beam is raster-scanned to record an average spectrum across a variable-size area, and the sample is moved by the motorized stage with a step matched to the scanned area size to cover the whole surface.

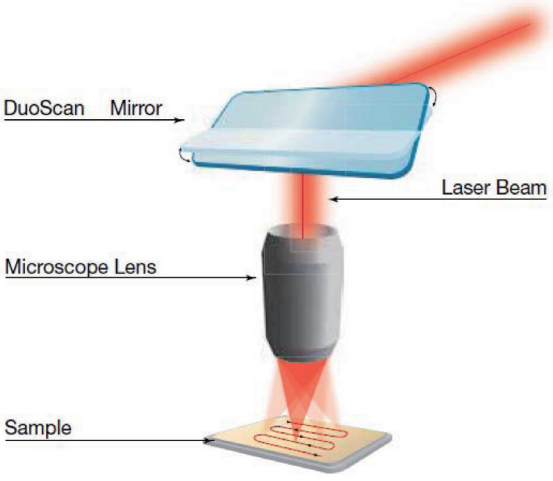

Figure 16 DuoScan principle of operation

Figure 17 LabRAM HR-AFM coupling system
The right picture shows the configuration of incident laser-radiation with 60 degrees angle at samples.

The Coupling System of Atomic Force Microscope (AFM) and Raman Mapping System

In step-by-step mapping mode, a sample area is selected and the sample is scanned point by point across the chosen area. The sample doesn't move, it is the laser that moves across the sample, making it possible to record fine mapping even on bulky or hard-to-move samples. The extreme accuracy of the scanning system, comparable to that of a piezo stage, allows stable and repeatable displacement of the laser beam down to 50 nm. Images can be generated in high definition for optimal resolution. HORIBA coupling system of Atomic Force Microscope (AFM) and Raman mapping system, as shown in Figure 17, is another progress to measure both topography and Raman imaging at the same area. The latest development is combination of Raman imaging with the DuoScan step-by-step mode of XploRA-INV and AFM systems in Figure 18. These systems are moving Raman imaging far into the sub-micron regime, making nanoscale Raman imaging a reality at last.

Figure 18 XploRA-INV coupled with AFM
Coupling Raman system with inverted microscope and AFM. The right picture shows the configuration at samples

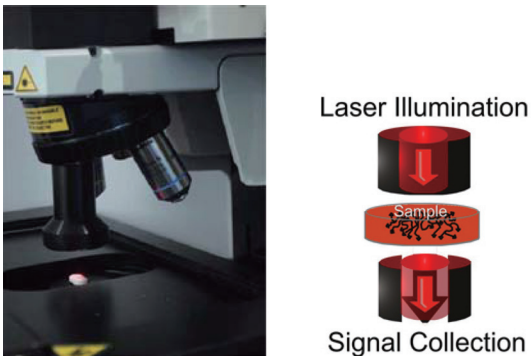

Figure 19 Transmission Raman accessory (left) and its signal correction system (right)

The Transmission Raman Spectroscopy (TRS)

TRS targets the collection of information about the bulk volume of a sample, because it analyses the light that traveled through the entire thickness of the sample (see Figure 19). It can be used for the analysis of component concentration, and, in particular, content uniformity. It also works for capsules and other materials outside of the pharmaceutical field such as biomaterials (tissues, food), polymers, or even geology. The Transmission Raman accessory is available for most of the HORIBA range of Raman microscope systems.

The Ultra-Low Frequency Raman Module[15]

With the introduction of the Ultra-Low Frequency (ULF) module (ICORS 2010), HORIBA Scientific now gives access to ultra-low frequency down to 5 cm^{-1} on the LabRAM HR. Traditionally low frequency analysis has been confined to large research systems or complex and expensive instruments such as Far IR or Terahertz spectrometers – now the ULF module for the LabRAM HR Raman microscope opens up this field to the routine analyst. The high throughput of the LabRAM HR series allows measurements to be obtained in just a few seconds or minutes. Moreover, Stokes and anti-Stokes spectral features can be simultaneously measured, providing additional information to the user (see Figure20).

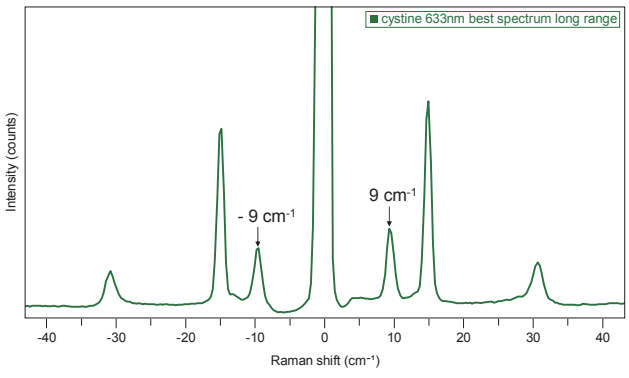

Figure 20 Very low frequency 9cm^{-1} band of L-Cystine measured with ULF

Figure 21 XploRA

The Raman Microscope XploRA

The Raman Microscope XploRA is a new concept in Raman microscopy bringing Raman chemical identification directly to optical microscope. Combining microscopy and chemical analysis the system retains the full functionality of microscope coupled with high performance Raman spectroscopy. Compact and rugged in design, the XploRA is easy to use and transport due to its minimal footprint, making it the ideal smart microscope for R&D, QA/QC and forensic lab. It makes it possible to explore the nature of samples with rapid compound identification and chemical imaging, with no sample preparation and at atmospheric conditions (see Figure 21).

The LabRAM HR Evolution

The LabRAM HR Evolution is the latest spectrometer in the proven LabRAM series. It is a flexible base unit which can be expanded with a range of options, upgrades and accessories to suit all applications. Specialized dedicated and/or customized solutions can be supplied where required whatever spectral resolution, laser wavelength or sampling regime is needed. Moreover, it ideally suited to both micro and macro measurements and offer advanced confocal imaging capabilities in 2D and 3D. The true confocal microscope enables the most detailed images of analyses to be obtained with speed and confidence (see Figure 22).

Figure 22 LabRAM HR Evolution

References

[1] M. Delhaye, M. Migeon, C. R. Acad, *Sc. Paris*., **262**, 702 (1966).
[2] M. Delhaye, M. Migeon, C. R. Acad, *Sc. Paris*., **262**, 1513 (1966).
[3] K. Buckley and P. Matousek, *J. Pharm*, *Biomed. Anal*., **55**, 645 (2011).
[4] J. Johansson, A. Sparén, O. Svensson, S. Folestad, and M. Claybourn, *Appl. Spectrosc*., **61**, 1211 (2007).
[5] F. Adar, *Spectroscopy*, pp.28-39, Feb 1, 2009, available online (http://www.spectroscopyonline.com/spectroscopy/article/articleDetail.jsp?id=583774)
[6] F. Tuinstra and J.L. Koenig, *J. Chem. Phys*., **53m**, 1126 (1970).
[7] Y. Wang, D.C. Alsmeyer, and R.L. McCreery, *Chem. Mater*., **2**, 557 (1990).
[8] A.C. Ferrari, *Solid State Commun*. **143**, 47 (2007), available online 27 April 2007.
[9] P.H. Tan, W.P. Han, W.J. Zhao, Z.H. Wu, K. Chang, H. Wang, Y.F. Wang, N. Bonini, N. Marzari, N. Pungo, G. Savini, A. Lombardo and A.C. Ferrari, *nature materials*, **2012** February
[10] T. Nagaura, K. Tozawa, *Prog. Batteries Solar Cells*, **9**, 209 (1990).
[11] T. Ohzuku, Y. Makimura, *Chem. Lett*., **30**, 642 (2001).
[12] V.A. Sethuraman, L.J. Hardwick, V. Srinivasan, R. Kostecki, *J. Power Sources*, **195**, 11, 3655 (2010).
[13] HORIBA Technical Note RA-TN01
[14] HORIBA Technical Note RA-TN04
[15] HORIBA Technical Note RA-TN02

Yasushi NAKATA
Manager
Application R&D Center
Research & Development Div.
HORIBA, Ltd.
Ph. D.

Emmanuel FROIGNEUX
Raman Product Manager
Sales & Marketing Div.
HORIBA Jobi Yvon S.A.S